

Linear Dimensions of Adsorbed Semiflexible Polymers: What can be learned about their persistence length?

Andrey Milchev^{1,2} and Kurt Binder²

¹*Institute for Physical Chemistry, Bulgarian Academy of Sciences, 1113, Sofia, Bulgaria and*

²*Institute of Physics, Johannes Gutenberg University Mainz, Staudingerweg 7, 55128 Mainz, Germany*

Conformations of partially or fully adsorbed semiflexible polymer chains are studied varying both contour length L , chain stiffness, κ , and the strength of the adsorption potential over a wide range. Molecular Dynamics simulations show that partially adsorbed chains (with “tails”, surface attached “trains” and “loops”) are not described by the Kratky-Porod wormlike chain model. The crossover of the persistence length from its three-dimensional value (ℓ_p) to the enhanced value in two dimensions ($2\ell_p$) is analyzed, and excluded volume effects are identified for $L \gg \ell_p$. Consequences for the interpretation of experiments are suggested. We verify the prediction that the adsorption threshold scales as $\ell_p^{-1/3}$.

PACS numbers:

Introduction Adsorbed stiff macromolecules on substrates are of key interest to understand properties and function of various nanomaterials, and also play an important role in biological context [1–7]. While adsorption of flexible polymers has been extensively studied [8–12], the adsorption transition of semiflexible polymers is much less understood [13–23]. For flexible polymers, the salient features of this transition are well captured [10–12] by the simple selfavoiding walk lattice model of polymers [24]. However, extending the model to semiflexible polymers [13, 20] misses important degrees of freedom, namely, chain bending [25] by small bending angle θ . Consequently, most work uses the Kratky-Porod (KP)[26] wormlike chain (WLC) model: in the continuum limit the chain is described by a curve $\vec{r}(s)$ in space, the only energy parameter κ considered relates to the local curvature of the polymer. The Hamiltonian

$$\frac{\mathcal{H}}{k_B T} = \frac{\kappa}{2} \int_0^L ds \left(\frac{d^2 \vec{r}(s)}{ds^2} \right)^2 \quad (1)$$

yields for the tangent - tangent correlation function an exponential decay with the distance n between two bond vectors ($n = s - s'$) along the chain backbone,

$$C(n) = \langle \cos \theta(n) \rangle = e^{-n/\ell_p} (d=3), \text{ or } e^{-n/2\ell_p} (d=2), \quad (2)$$

with $\ell_p = \kappa$ the persistence length. There are two problems: (i) while in $d = 3$ dimensions excluded volume interactions between the effective monomer units of the polymer come into play only for extremely long chains when $\ell_p \gg 1$ (measuring lengths in units of the distance $\ell_b = 1$ between the subsequent monomers along the chain) [27], in $d = 2$ deviations from Eq.(2) start when $s - s'$ exceeds $2\ell_p$ distinctly, and a gradual crossover to a power-law decay, $\langle \cos \theta(s - s') \rangle \propto (s - s')^{-\beta}$ with $\beta = 2(1 - \nu) = 1/2$ [28] begins. Strictly in $d = 2$, chains cannot intersect, and for $L \gg \ell_p$ excluded volume matters. (ii) in fact, adsorbed chains exist to some extent “in between” the dimensions (remember the well-known [11] description in terms of trains, tails and loops, cf.

Fig.1a: tails and loops exists in $d = 3$, trains reside (almost) in $d = 2$). If the adsorption potential, $U(z)$, with z being the distance from the (planar) adsorbing substrate, is very strong, tails and loops will be essentially eliminated but in real systems the adsorption then must be expected to be irreversible[29]. While single-stranded (ss)-DNA on graphite [7] and double-stranded (ds)-DNA on lipid membranes [6] have been shown to equilibrate by diffusion in the adsorbed state, no diffusion is observed for more bulky polymers such as dendronized polymers (DP) [30]. Adsorbed bottlebrush polymers [31] or DPs are intriguing since ℓ_p for such polymers can be systematically varied by choosing different side chain lengths (for bottlebrushes [32]), or different generations (for DPs [30, 33, 34]). However, experiments reveal subtle effects of surface roughness [30] and electrostatic interactions [30] making thus the interpretation of the observed persistence lengths difficult.

Model In the present work we elucidate the meaning of ℓ_p for experimentally observed semiflexible polymers by means of Molecular Dynamics simulations using a bead-spring model as studied previously in both $d = 2$ [35] and in $d = 3$ [36], assuming dilute solutions under good solvent conditions. All beads interact with a truncated and shifted Lennard-Jones potential,

$$U_{LJ}(r) = 4\epsilon \left[\left(\frac{\sigma}{r} \right)^{12} - \left(\frac{\sigma}{r} \right)^6 + \frac{1}{4} \right], \quad (3)$$

where $U_{LJ} = 0$ for distances $r > 2^{1/6}\sigma$, ϵ being chosen as unity, $\epsilon = k_B T = 1$, and the range $\sigma = 1$. Eq.(3) therefore means that excluded volume effects are fully accounted for. Chain connectivity is ensured by the finitely extensible nonlinear elastic (FENE) potential [37], $U_{FENE}(r) = -(1/2)kR_0^2 \ln(1 - r^2/R_0^2)$, with $R_0 = 1.5\sigma$, $k = 30$ (the average bond length ℓ_b is then roughly 0.976). The bond bending potential is taken as $U_b = \kappa(1 - \cos \theta) \approx \frac{1}{2}\kappa\theta^2$, compatible with Eq.(1), θ being the angle between subsequent bonds.

A popular measure of ℓ_p then is [32] $\ell_b/\ell_p = -\ln \langle \cos \theta \rangle \approx \frac{1}{2} \langle \theta^2 \rangle$, for $\kappa \gg 1$. This relationship yields

the results displayed in Fig.1b, i.e., $\ell_p/\ell_b \approx \kappa$, irrespective of the chosen substrate potential

$$U_{wall}(z) = \epsilon_{wall} \left(\frac{5}{3}\right) \left(\frac{5}{2}\right)^{\frac{2}{3}} \left[\left(\frac{\sigma}{z}\right)^{10} - \left(\frac{\sigma}{z}\right)^4 \right], \quad (4)$$

which has a minimum $U_{wall}(z_{min}) = -\epsilon_{wall}$ at $z_{min}/\sigma = (\frac{5}{2})^{1/6}$. In the simulations below, varying ϵ_{wall} and the chain length N , we have carefully monitored that on the available time scale (of the order of up to 10 million MD time units) equilibrium is reached. In each case 50 runs (carried out in parallel using graphics processing unit) were averaged over.

Results While for small ϵ_{wall} the chains are essentially non-adsorbed mushrooms (one chain end being fixed at

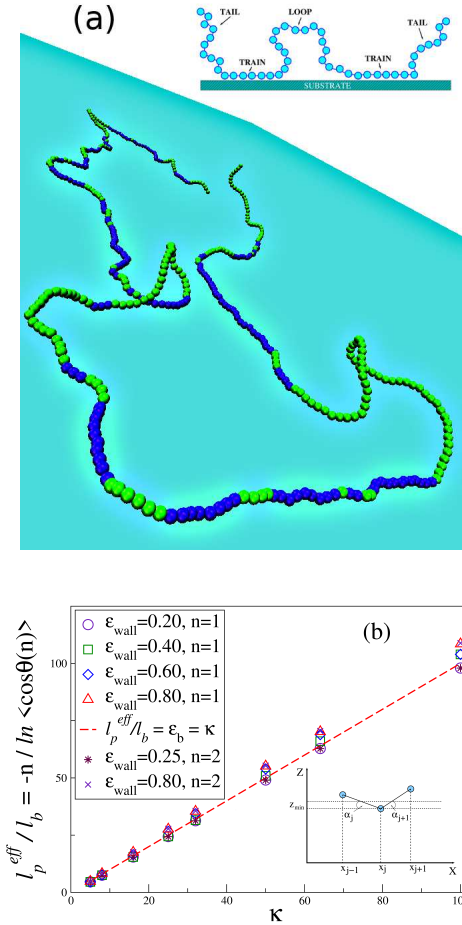


FIG. 1: (a) Snapshot of an adsorbed chain with $N = 500$ for $\kappa = 16, \epsilon_{wall} = 0.65$. Loops and a tail are shown in green, trains are in darkblue. (b) Decay length ℓ_p^{eff}/ℓ_b vs stiffness κ for $N = 250$ and several choices of ϵ_{wall} . Here $n = 1$ means an angle between nearest bonds, $n = 2$ stands for next-nearest bonds. Data for $n = 1, 2$ indicate that ℓ_p^{eff} increases rather gradually with κ for adsorbed chains. The inset illustrates the geometry of the x, z -coordinates of two subsequent bonds where the X -axis is chosen such that the bond from \vec{r}_{j-1} to \vec{r}_j lies in the X, Z plane. The angles $\alpha_j = \frac{\pi}{2} - \vartheta_j$ are the complements to the polar angles ϑ_j of the bonds with the Z -axis.

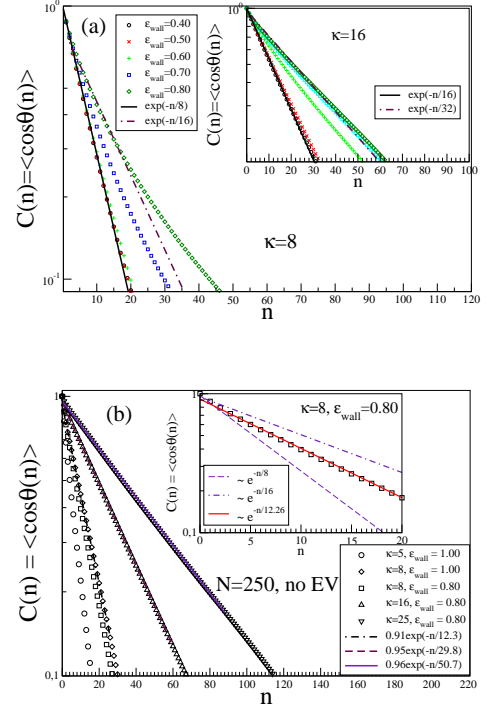


FIG. 2: (a) Semilog plot of $C(n) = \langle \cos \theta(n) \rangle$, vs n in semi-log coordinates for $\kappa = 8$ (main panel) and $\kappa = 16$ (inset). Several choices of ϵ_{wall} are shown, as indicated. All data are for $N = 250$. (b) The same as in (a) but for strongly adsorbed ($\epsilon_{wall} = 0.80, 1.00$) chains with stiffness $\kappa = 5, 8, 16, 25$ without EV interactions. The inset indicates the gradual crossover in the decay of $C(n)$ with n for $\kappa = 8$ and $n = 1, 2$ from $\ell_p^{eff} \approx 8$ to $\ell_p^{eff} = 12.3$ for large n .

the surface), for $\epsilon_{wall} \approx 1.0$ all monomers are bound to the wall, i.e., a quasi-two-dimensional conformation occurs. Surprisingly, for neighboring bonds, $s - s' = 1$, the expected change of the effective decay length ℓ_p^{eff} of orientational correlations from ℓ_p to $2\ell_p$ ($2\ell_p$ is readily seen for strictly $d = 2$ chains [35]) is *not* observed.

This finding is rationalized by considering two subsequent bonds, the first bond from \vec{r}_{j-1} to \vec{r}_j , the second from \vec{r}_j to \vec{r}_{j+1} , (cf. inset to Fig.1b). Choosing polar coordinates to describe the bonds $\vec{r}_j - \vec{r}_{j-1} = \ell_b(-\cos \alpha_j, 0, \sin \alpha_j)$ and $\vec{r}_{j+1} - \vec{r}_j = \ell_b(\cos \alpha_{j+1} \cos \phi, \cos \alpha_{j+1} \sin \phi, \sin \alpha_{j+1})$, for small angles θ between the bonds one has $\theta^2 = \phi^2 + (\alpha_j - \alpha_{j+1})^2$, therefore, also for an adsorbed polymer the bond angle θ is composed from *two* transverse degrees of freedom. Only if the wall potential would constrain all positions $\{z_j\}$ strictly to z_{min} , one would get $\alpha_j - \alpha_{j+1} \equiv 0$, that is, a *single* transverse degree of freedom. There are slight deviations from the result $\ell_p/\ell_b = \kappa$ in Fig.1b. However, when one follows $\langle \cos \theta(n) \rangle$ for large distances n along the contour, Fig.2a, one reproduces Eq.(2) strictly only for the non-adsorbed mushrooms, for all the weakly adsorbed chains, instead, the strong curvature of the semilog plot shows that an interpretation by Eq.(2) with a single decay length is inadequate. While quantitative details in Figs.1, 2 depend on the specific chain model and

the wall potential, the fact that $\langle \cos \theta(n) \rangle$ is not compatible with Eq.(2) for weakly adsorbed chains even at large n , and for strongly adsorbed chains applies only if both ℓ_p and n are large, is a generic feature. For strongly adsorbed chains a crossover of the effective decay length ℓ_p to about $2\ell_p$ occurs when n is significantly larger than 1. The further crossover to the power law [28] $C(n) \propto n^{-1/2}$ for $n \gg 2\ell_p$ in Fig. 2a sets in slowly, the fully developed power law is not seen here, it would require to study by far longer chains. To separate the EV effect from the crossover $\ell_p \rightarrow 2\ell_p$ caused by adsorption, we simulate chains where Eq.(3) between non-bonded monomers was omitted, Fig.2b. One sees that ℓ_p^{eff} reaches the value $2\ell_p$ only for large κ .

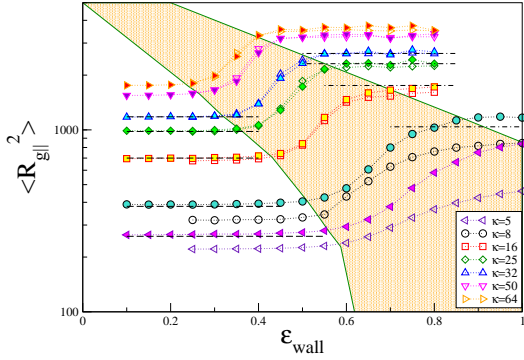


FIG. 3: Mean-square lateral gyration radius for $N = 250$ vs ϵ_{wall} for 7 choices of κ with (full symbols) and without (open symbols) excluded volume (EV) interactions. EV is more important for small κ ($\kappa = 5, 8$). Horizontal straight lines show KP predictions for $d = 3$ (for small ϵ_{wall}) and $d = 2$ (for larger ϵ_{wall}). The shaded transition region from non-adsorbed to adsorbed chains narrows down with growing κ .

The gradual crossover from e^{-n/ℓ_p} to $e^{-n/2\ell_p}$ with increasing ϵ_{wall} , and the precise range of ϵ_{wall} where this occurs, reflect the region over which the adsorption transition is rounded (owing to the finite chain length N) and depend on κ as well. The rounded transition is monitored by studying the lateral chain linear dimensions, Fig.3, or local order parameters, the fraction f of adsorbed monomers, defined by $f = \int \rho(z) U_{wall}(z) dz / \int U_{wall}(z) dz$, Fig.4a, or the orientational order parameter of the bonds $\eta = \frac{3}{2} \langle \cos^2 \vartheta \rangle - \frac{1}{2}$, ϑ being the angle of a bond with the surface normal, Fig.4b. For the shown medium chain lengths, EV effects for non-adsorbed chains are negligible for all κ . They are, however, present for $N = 100$ for adsorbed chains with $\kappa = 5$ and 8 whereas for $N = 250$ also data for adsorbed chains with $\kappa = 16$ and $\kappa = 25$ are already slightly affected by excluded volume. These findings are certainly compatible with experiment: for ss-DNA with $\ell_p \approx 4.6$ to $9.1 nm$, depending on the ion concentration in the solution, evidence for $\langle R^2(s) \rangle \propto s^{2\nu}$ with $\nu = 0.73$ was presented [7], in contrast to the KP prediction $\langle R^2(s) \rangle \propto \ell_p s$. Even

for long enough ds-DNA with $\ell_p = 50 nm$ (with effective diameter $\sigma = 2 nm$, this would correspond to $\kappa = 25$ in our model), the $d = 2$ SAW-type behavior was observed clearly [6]. Thus, the suggestion [4] to estimate ℓ_p from the KP expression by means of AFM measurement on DNA in the limit $L \gg \ell_p$ must be taken with due care since significant systematic errors may occur when both L and ℓ_p are used as adjustable parameters.

Fig.3 also includes a rough estimate of the lateral part of the mean-square gyration radius of non-adsorbed mushrooms ($\langle R_{gy}^2 \rangle \equiv \langle R_{gx}^2 \rangle + \langle R_{gy}^2 \rangle \approx 2/3 \langle R_g^2 \rangle_{d=3}^{KP}$ (with $\langle R_g^2 \rangle_{d=3}^{KP}$ being the result of the KP model in $d = 3$). For large ϵ_{wall} , the data roughly converge towards the corresponding predictions in $d = 2$ dimensions $\langle R_g^2 \rangle_{d=2}^{KP}$ (provided κ is large enough too). Denoting $n_p \equiv N/\ell_p$ (where ℓ_p is the $d = 3$ persistence length), one has in $d = 2$:

$$\frac{3 \langle R_g^2 \rangle}{2 \ell_p L} = 1 - \frac{6}{n_p} \left\{ 1 - \frac{4}{n_p} \left[1 - \frac{4}{n_p} \left(1 - \frac{1 - \exp(-n_p/2)}{n_p/2} \right) \right] \right\}, \quad (5)$$

whereas in $d = 3$ the same expression holds yet with ℓ_p being replaced by $\ell_p/2$ (also in n_p).

It is clear from Fig.3 that the KP model, Eq.(5), is inapplicable in the broad (shaded) transition region from weakly to strongly adsorbed chains. The chain conformations contain here large loops (whereby ℓ_p appropriate for $d = 3$ applies) as well as some trains (where $\ell_p^{eff} \approx 2\ell_p$). But even if the chains are so strongly adsorbed that loops no longer occur, ℓ_p^{eff} is less than $2\ell_p$ for intermediate values of κ , as Fig.2b shows: A decay law $C(n) = A \exp(-n/\ell_p^{eff})$ is observed, with $A < 1$ and $\ell_p^{eff} < 2\ell_p$. Using these results to modify Eq.(5), we can account for the actual values of $\langle R_g^2 \rangle$ in the strongly adsorbed regime shown in Fig.3 for those chains where EV is switched off. Thus, e.g., for $\kappa = 8, \epsilon_{wall} = 1, N = 250$, Eq.(5) would yield a $\langle R_g^2 \rangle$ of 1039 while the observation is about 847 only. Taking into account that $n_p^{eff} = 36.55$ instead of $n_p = 31.125$, and the reduction by $A = 0.93$ (see Fig.2b), we predict 845, in very good agreement with the simulation. Of course, for such not very stiff and rather long chains the complete neglect of excluded volume is not warranted, as $R_g^2 = 1167$ for the chain with EV shows. As seen in Fig.2a, EV also causes onset of curvature in the semilog plot of $C(n)$. Thus Gaussian statistics as implicit in the KP model for $L \gg \ell_p$ is clearly inadequate. Only for all the data without EV, the modified KP model (with ℓ_p^{eff} rather than $2\ell_p$) can account for the results qualitatively.

Since the adsorption transition becomes a well-defined (sharp) phase transition only for $N \rightarrow \infty$, and then the theory predicts[17] that $f \propto (\epsilon_{wall} - \epsilon_{wall}^{cr})$ for $\epsilon_{wall}^{cr} < \epsilon_{wall} < \epsilon_{wall}^{sat}$ for semiflexible polymers, we plot f vs ϵ_{wall} in Fig.4a for N extending from $N = 50$ to $N = 500$. Indeed, the data are qualitatively compatible with this prediction, and the estimates, ϵ_{wall}^{cr} , thus obtained comply within error bars with the predicted[17] behavior $\epsilon_{wall}^{cr}/k_B T \propto (\ell_p/\ell_b)^{-1/3} = \kappa^{-1/3}$, cf. Fig.4c. This is understood qualitatively by decomposing the adsorbed

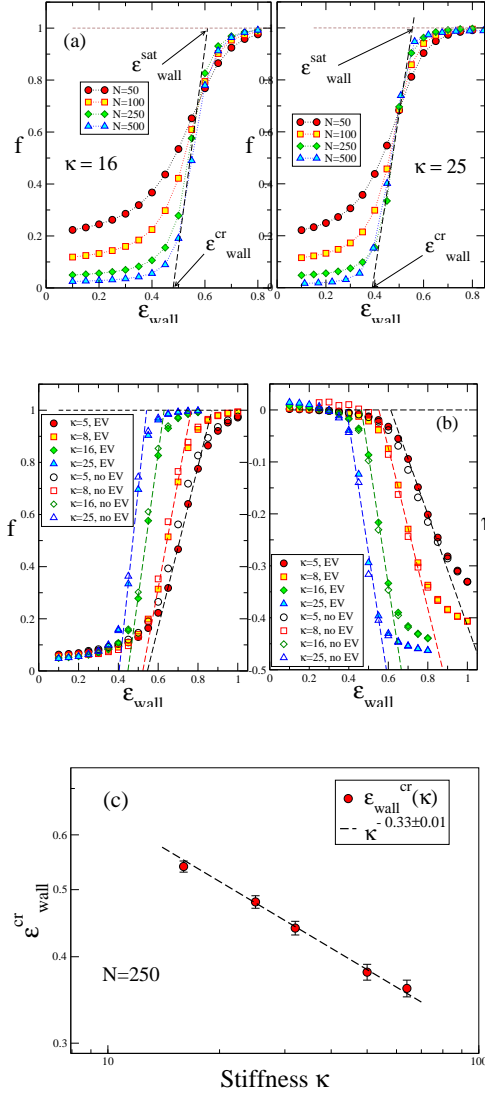


FIG. 4: (a) Fraction f of adsorbed monomers vs ϵ_{wall} for $\kappa = 16$ (left panel) and $\kappa = 25$ (right panel), for the 4 chain lengths $N = 50, 100, 250$ and 500 , respectively. Tentative linear extrapolations indicate the estimated location of the adsorption transition, ϵ_{wall}^{cr} , (nonzero f for $\epsilon_{wall} < \epsilon_{wall}^{cr}$ is a finite-size effect). Also the estimation of ϵ_{wall}^{sat} , where f crosses over to saturation value $f = 1$, is indicated. (b) Adsorbed fraction f plotted vs ϵ_{wall} for $N = 250$ and 4 choices of κ (left), and orientational order parameter of the bonds $\eta = \frac{3}{2}\langle \cos^2 \vartheta \rangle - \frac{1}{2}$ vs ϵ_{wall} (right). Data with no EV interaction (open symbols) are also included. (c) Variation of the critical adsorption potential ϵ_{wall}^{cr} with chain stiffness κ for $N = 250$.

chain into straight pieces of length $\lambda \propto \ell_p^{1/3} \Delta^{2/3}$, Δ being the range of the adsorption potential while λ is the “deflection length” [25]. The transition occurs when the energy won by one such piece is of order $k_B T$. Fig. 4a also shows estimates of ϵ_{wall}^{sat} where f gradually reaches saturation, $f \rightarrow 1$. However, while with increasing κ the curves f vs ϵ_{wall} do become steeper, we are still far from the 1st-order-like behavior, predicted [17] for $\kappa \rightarrow \infty$.

Conclusions In summary, using a bead-spring model with a bond-angle potential where the nonbonded part of the excluded volume potential between monomers is either included or switched off, a test of the KP description of the adsorption of semiflexible polymers is presented. Unlike previous lattice model work (predicting $\epsilon_{wall}^{cr} \propto 1/\ell_p$), we verify Semenov’s [17] prediction $\epsilon_{wall}^{cr} \propto 1/\ell_p^{1/3}$. Ref. [17] presents a precise description of the adsorption of ideal wormlike (KP) chains and explains why previous attempts (apart from considerations based on the unbinding transitions [16]) failed. While near the transition (for very stiff chains) excluded volume is unimportant, it matters for strongly adsorbed quasi-2d chains. We show that the concept of persistence length is not useful for weakly adsorbed chains, and for the strongly adsorbed chains we demonstrate that the $\ell_p \rightarrow 2\ell_p$ change, predicted by the KP model, only holds for very large ℓ_p . We expect that these findings will help the proper interpretation of experiments on adsorbed ss-DNA and ds-DNA.

Acknowledgements A.M. is indebted to the Alexander von Humboldt foundation for financial support during this study and also thanks the COST action No. CA17139, supported by COST (European Cooperation in Science and Technology [38]) and its Bulgarian partner FNI/MON under KOST-11.

[1] P. A. Wiggins, T. van der Heijden, F. Moreno-Herrero, A. Spakowitz, R. Phillips, J. Widom, C. Dekker, and P. C. Nelson, *Nature Nanotechnology* **1**, 137 (2006)
[2] L. Han, H. G. Garcia, S. Blumberg, K. B. Towles, J. F. Beausang, P. C. Nelson, R. Phillips, *PLOS One* **4**, e5621 (2009)
[3] E. Vafabaksch and T. Ha, *Science* **337**, 1097 (2012)
[4] J. Moukhtar, E. Fontaine, C. Faivre-Moskalenko, and A.

Arneodo, *Phys. Rev. Lett.* **98**, 178101 (2007)
[5] J. Moukhtar, C. Faivre-Moskalenko, P. Milani, B. Audit, C. Vaillant, E. Fontaine, F. Mongelar, G. Lavorel, P. St-Jean, P. Bouvet, F. Argoul, and Alain Arneodo, *J. Phys. Chem. B* **114**, 5125 (2010)
[6] B. Maier and J. O. Rädler, *Phys. Rev. Lett.* **82**, 1911 (1999)
[7] K. Rechendorff, G. Witz, J. Adamcik, and G. Dietler, J.

- Chem. Phys. **131**, 095103 (2009)
- [8] R. Sinha, H. L. Frisch, and F. R. Eirich, J. Chem. Phys. **57**, 584 (1953)
 - [9] P. G. de Gennes, Macromolecules **14**, 1637 (1981)
 - [10] E. Eisenriegler, K. Kremer, and K. Binder, J. Chem. Phys. **77**, 6296 (1982)
 - [11] G. J. Fleer, M. A. Cohen Stuart, J. M. H. M. Scheutjens, T. Cosgrove, and B. Vincent, *Polymers at Interfaces* (Chapman and Hall, London, 1993)
 - [12] L. I. Klushin, A. A. Polotsky, H.-P. Hsu, D. A. Markelov, K. Binder, and A. M. Skvortsov, Phys. Rev. E **87**, 022604 (2013)
 - [13] T. M. Birshtein, E. B. Zhulina, A. M. Skvortsov, Biopolymers **18**, 1171 (1979)
 - [14] A. R. Khokhlov, F. F. Ternovsky, and E. A. Zheligovskaya, Macromol. Chem. Theory Simul. **2**, 151 (1993)
 - [15] E. Yu. Kramarenko, R. G. Winkler, P. G. Khalatur, A. R. Khokhlov, and P. Reineker, J. Chem. Phys. **104**, 4806 (1996)
 - [16] A. C. Maggs, D. A. Huse, and S. Leibler, Europhys. Lett. **8**, 615 (1989)
 - [17] A. N. Semenov, Eur. Phys. J. E **9**, 353 (2002)
 - [18] R. R. Netz and D. Andelman, Phys. rep. **380**, 1 (2003)
 - [19] M. Deng, Y. Jiang, H. Liang, and J. Z. Y. Chen, J. Chem. Phys. **133**, 034902 (2010)
 - [20] H.-P. Hsu and K. Binder, Macromolecules, **46**, 2496 (2013)
 - [21] T. A. Kampmann, H. H. Boltz, and J. Kierfeld, J. Chem. Phys. **139**, 034903 (2013)
 - [22] J. Baschnagel, H. Meyer, J. Wittmer, I. Kulić, H. Mohrbach, F. Ziebert, G.-M. Nam, N.-K. Lee, and A. Johner, Polymers **8**, 286 (2016)
 - [23] T. A. Kampmann and J. Kierfeld, J. Chem. Phys. **147**, 014901 (2017)
 - [24] A. Grosberg and A.R. Khokhlov, *Statistical Physics of Macromolecules* (AIP Press, New York, 1994)
 - [25] T. Odijk, Macromolecules, **16**, 1340 (1983)
 - [26] O. Kratky and G. Porod, J. Colloid Sci., **4** 35 (1949)
 - [27] H.-P. Hsu, W. Paul, and K. Binder, EPL **92**, 28003 (2010)
 - [28] H.-P. Hsu, W. Paul, and K. Binder, EPL **95**, 68004 (2011)
 - [29] N.-K. Lee and A. Johner, Macromolecules **48**, 7681 (2015)
 - [30] L. Grebikova, S. Kozhuharov, P. Maroni, A. Mikhaylov, G. Dietler, A. D. Schlüter, M. Ullnerd, and M. Borkovec, Nanoscale **8**, 13498 (2016)
 - [31] H.-P. Hsu, W. Paul, and K. Binder, J. Chem. Phys. **133**, 134902 (2010)
 - [32] H.-P. Hsu, W. Paul, and K. Binder, Macromolecules **43**, 3094 (2010)
 - [33] D. Messner, Christoph Böttcher, H. Yu, A. Halperin, Kurt Binder, Martin Kröger, and A. D. Schlüter, ACS NANO, **13**, 3466 (2019)
 - [34] F. Dutertre, Ki-Taek Bang, E. Vereroudakis, B. Lopinet, Sanghee Yang, Sung-Yun Kang, George Fytas, and Tae-Lim Choi, Macromolecules **52**, 3342 (2019)
 - [35] A. Huang, H.-P. Hsu, Aniket Bhattacharya, and K. Binder, J. Chem. Phys. **143**, 243102 (2015)
 - [36] S. A. Egorov, A. Milchev, P. Virnau, and K. Binder, Soft Matter **12**, 4944 (2016)
 - [37] G. S. Grest and K. Kremer, Phys. Rev. A **33**, 3628 (1986)
 - [38] See <http://www.cost.eu> and <https://www.fni.bg>